

Enhancement of the $\bar{\nu}_e$ flux from astrophysical sources by two photon annihilation interactions

Soebur Razzaque,^{1,2} Peter Mészáros^{1,2} and Eli Waxman³

¹*Department of Astronomy & Astrophysics, Pennsylvania State University, University Park, PA 16802, USA*

²*Department of Physics, Pennsylvania State University, University Park, PA 16802, USA and*

³*Physics Faculty, Weizmann Institute of Science, Rehovot 76100, Israel*

(Dated: December 15, 2018)

The ratio of anti-electron to total neutrino flux, $\Phi_{\bar{\nu}_e} : \Phi_\nu$, expected from $p\gamma$ interactions in astrophysical sources is $\leq 1 : 15$. We point out that this ratio is enhanced by the decay of $\mu^+\mu^-$ pairs, created by the annihilation of secondary high energy photons from the decay of the neutral pions produced in $p\gamma$ interactions. We show that, under certain conditions, the $\Phi_{\bar{\nu}_e} : \Phi_\nu$ ratio may be significantly enhanced in gamma-ray burst (GRB) fireballs, and that detection at the Glashow resonance of $\bar{\nu}_e$ in kilometer scale neutrino detectors may constrain GRB fireball model parameters, such as the magnetic field and energy dissipation radius.

PACS numbers: 96.40.Tv, 14.60.Pq, 98.70.Rz, 98.70.Sa

I. INTRODUCTION

High energy neutrinos are expected to be produced in astrophysical sources mainly by $p\gamma$ interactions, leading to the production and subsequent decay of charged pions: $\pi^+ \rightarrow e^+\nu_e\bar{\nu}_\mu\nu_\mu$ (see, e.g., [1] for recent reviews). Neutrino oscillations lead in this case to an observed ratio of $\bar{\nu}_e$ flux to the total ν flux of $\simeq 1 : 15$ [2] (or lower, in case muons suffer significant electromagnetic energy loss prior to decay [3]). For neutrinos produced in inelastic pp (pn) nuclear collisions, where both π^+ 's and π^- 's are produced, the ratio is $\simeq 1 : 6$, and it was suggested that measurements of the ν_e to $\bar{\nu}_e$ flux ratio at the W -resonance may allow one to probe the physics of the sources by discriminating between the two primary modes of pion production, $p\gamma$ and pp collisions [4]. This test for discriminating between the two mechanisms is complicated by the fact that the ratio of $\Phi_{\bar{\nu}_e}$ to Φ_ν produced in $p\gamma$ interactions can be enhanced to a value similar to that due to inelastic nuclear collisions in sources where the optical depth to $p\gamma$ interactions is large (e.g. [3]). In this case, neutrons produced in $p\gamma \rightarrow n\pi^+$ interactions are likely to interact with photons and produce π^- before escaping the source, leading to production of roughly equal numbers of π^+ 's and π^- 's.

In this paper, we point out that the $\Phi_{\bar{\nu}_e} : \Phi_\nu$ ratio from $p\gamma$ interactions may be enhanced above $1 : 15$ also in sources with small $p\gamma$ optical depth. Neutral pions, which are created at roughly the same rate as charged pions in $p\gamma$ interactions, decay to produce high energy γ -rays. These γ -rays typically carry $\sim 10\%$ of the initial proton energy, and may therefore interact with the low energy photons (with which the protons interact to produce pions) to produce $\mu^+\mu^-$ pairs. The decay of muons yields (after vacuum oscillations) $\Phi_{\bar{\nu}_e} : \Phi_\nu \simeq 1 : 5$, thus enhancing the $\bar{\nu}_e$ fraction.

We discuss below a specific example, the widely considered fireball model of GRBs. In this model, the observed γ -rays are produced by synchrotron radiation of shock accelerated electrons in the magnetic field which is as-

sumed to be a fraction of the total energy (see [5] e.g. for reviews). The protons are expected to co-accelerate with electrons to ultra-high energy [6], and produce high energy neutrinos by $p\gamma$ interactions [7]. We calculate below the additional neutrino flux, due to the decay of muons produced by secondary photon annihilation, for a typical long duration GRB, and show that the enhanced $\bar{\nu}_e$ flux may be detectable at the Glashow resonance ($\bar{\nu}_e e \rightarrow W^- \rightarrow \text{anything}$ [8]) in kilometer scale neutrino detectors such as IceCube [9].

The enhancement of $\Phi_{\bar{\nu}_e} : \Phi_\nu$ due to $\gamma\gamma$ interactions in $p\gamma$ sources makes the discrimination between $p\gamma$ and pp neutrino sources more difficult. On the other hand, it may provide a new handle on the physics of the source. We show below that for GRBs the enhancement of $\bar{\nu}_e$ flux depends on model parameters which are poorly constrained by observations, namely the magnetic field strength and the energy dissipation radius. Detection of $\bar{\nu}_e$'s at the Glashow resonance, in conjunction with γ -ray detection, may therefore constrain these parameters.

II. FIREBALL MODEL AND PHOTON SPECTRUM

The minimum observed GRB fireball radius r may be estimated by requiring that it is optically thin to Thomson scatterings: $\tau'_{\text{Th}} = \sigma_{\text{Th}} n' r' \lesssim 1$ (denoting the comoving and local lab. frame variables with and without a prime respectively). Here n' is the density of scatterers in the fireball, $r' = r/\Gamma$ is the size of the interaction region and Γ is the bulk Lorentz factor. The radius at which $\tau'_{\text{Th}} \approx 1$ is the photospheric radius r_{ph} . For a kinetic luminosity L_k of the fireball, mostly carried by the baryons, the number density of the baryons, and of the leptons which are coupled to the baryons, is $n'_b \approx L_k / (4\pi r'^2 \Gamma^2 m_p c^3)$. The observed isotropic equivalent γ -ray luminosity of a long duration GRB is $L_{52} = L_\gamma / 10^{52} \text{erg/s} \sim 1$. Assuming $L_\gamma = \epsilon_e L_k$ with $\epsilon_e \sim 0.05\epsilon_{e,-1.3}$ (a parametrization which is moti-

vated below), the photospheric radius is

$$r_{\text{ph}} = \frac{\sigma_{\text{Th}} L_{\gamma} / \varepsilon_e}{4\pi \Gamma^3 m_p c^3} \approx 7.4 \times 10^{12} \frac{L_{52}}{\varepsilon_{e,-1.3} \Gamma_{2.5}^3} \text{ cm}, \quad (1)$$

for $\Gamma_{2.5} = \Gamma/316 \sim 1$. The radius at which the bulk kinetic energy dissipation occurs, e.g. by internal shocks, is in general $r \gtrsim r_{\text{ph}}$.

The γ -ray spectrum of a GRB fireball at a dissipation radius $r = 10^{14} r_{14}$ cm peaks at a typical energy

$$\begin{aligned} \epsilon_{\gamma, \text{pk}} &= \hbar c \Gamma^2 (3\gamma'_{e, \text{min}} q B') / (2m_e c^2) \\ &\sim 500 (\varepsilon_{e,-1.3}^3 \varepsilon_{B,-1} L_{52} \Gamma_{2.5}^2 / r_{14}^2)^{1/2} \text{ keV}, \end{aligned} \quad (2)$$

due to synchrotron radiation by electrons with a Lorentz factor $\gamma'_{e, \text{min}} \approx \varepsilon_e (m_p/m_e)$. Here, $\gamma'_{e, \text{min}}$ is at the lower end of a $\propto 1/\gamma_e^p$ distribution of electron Lorentz factor, with $p \gtrsim 2$, created by Fermi acceleration in the shock. The magnetic field is assumed to be $B'^2/8\pi \approx \varepsilon_B L_k / (4\pi r^2 \Gamma^2 c)$, where $\varepsilon_B \sim 0.1 \varepsilon_{B,-1}$ is the equipartition value, currently unconstrained in the GRB prompt phase. Note that $\epsilon_{\gamma, \text{pk}} \propto 1/r$ will be larger than the above value for $r \approx r_{\text{ph}}$, with other parameters fixed.

For a GRB at a luminosity distance d_L the observed γ -ray spectrum is generally approximated with a broken power-law Band fit [10],

$$\frac{dN_{\gamma}}{d\epsilon_{\gamma}} \approx \frac{L_{\gamma}}{4\pi d_L^2 \epsilon_{\gamma, \text{pk}}^2} \begin{cases} (\epsilon_{\gamma}/\epsilon_{\gamma, \text{pk}})^{-1} ; & \epsilon_{\gamma} < \epsilon_{\gamma, \text{pk}} \\ (\epsilon_{\gamma}/\epsilon_{\gamma, \text{pk}})^{-2} ; & \epsilon_{\gamma} > \epsilon_{\gamma, \text{pk}} \end{cases} \quad (3)$$

The spectrum deviates from this at low energy, becoming $dN_{\gamma}/d\epsilon_{\gamma} \propto \epsilon_{\gamma}^{3/2}$ for $\epsilon_{\gamma} \lesssim \epsilon_{\gamma, \text{sa}}$, the energy below which synchrotron self-absorption becomes dominant. Theoretical modeling indicates a value [11]

$$\begin{aligned} \epsilon_{\gamma, \text{sa}} &\approx 2.4 \left(\Gamma^2 \gamma'_{e, \text{min}} n'_e r [q \hbar c]^4 B'^2 / [m_e^3 c^6] \right)^{1/3} \\ &\sim 8 (\varepsilon_{B,-1} L_{52}^2 / [\varepsilon_{e,-1.3} \Gamma_{2.5}^2 r_{14}^3])^{1/3} \text{ keV}, \end{aligned} \quad (4)$$

for $p = 2$. The differential number density of photons is

$$\begin{aligned} dN'_{\gamma}/d\epsilon'_{\gamma} &\approx L_{\gamma} / (4\pi r^2 c \epsilon_{\gamma, \text{pk}}^2) \\ &\times \begin{cases} \left(\epsilon'_{\gamma, \text{sa}} / \epsilon'_{\gamma, \text{pk}} \right)^{-1} (\epsilon'_{\gamma} / \epsilon'_{\gamma, \text{sa}})^{3/2} ; & \epsilon'_{\gamma} < \epsilon'_{\gamma, \text{sa}} \\ \left(\epsilon'_{\gamma} / \epsilon'_{\gamma, \text{pk}} \right)^{-1} ; & \epsilon'_{\gamma, \text{pk}} > \epsilon'_{\gamma} > \epsilon'_{\gamma, \text{sa}} \\ \left(\epsilon'_{\gamma} / \epsilon'_{\gamma, \text{pk}} \right)^{-2} ; & \epsilon'_{\gamma} > \epsilon'_{\gamma, \text{pk}} \end{cases} \end{aligned} \quad (5)$$

Electron synchrotron radiation produces a power law γ -ray spectrum at energies above $\epsilon_{\gamma, \text{pk}}$ [see Eq. (2)] which depends on the maximum Lorentz factor. Other mechanisms can contribute to an extension of the γ -ray spectrum in Eq. (3) to high energies. High energy electrons can inverse Compton scatter synchrotron photons up to an energy similar to the maximum shock accelerated electron energy (which we derive shortly) in the Klein-Nishina limit in one mechanism. Here we consider

ultra-high energy γ -rays from π^0 decays which are produced by $p\gamma$ interactions of shock accelerated protons with synchrotron photons as $p\gamma \rightarrow \Delta^+ \rightarrow p\pi^0 \rightarrow p\gamma\gamma$.

The maximum proton energy is calculated by equating its acceleration time $t'_{\text{acc}} \approx \epsilon'_p / (q c B')$ to the shorter of the dynamic time $t'_{\text{dyn}} \approx r / (2\Gamma c)$ and the synchrotron cooling time $t'_{\text{syn}} \approx 6\pi m_p^4 c^3 / (\sigma_{\text{Th}} m_e^2 \epsilon'_p B'^2)$ as

$$\begin{aligned} \epsilon_{p, \text{max}} &= (6\pi m_p^4 c^4 q \Gamma^2 / [\sigma_{\text{Th}} m_e^2 B'])^{1/2} \\ &\approx 3.3 \times 10^{11} (\varepsilon_{e,-1.3} \Gamma_{2.5}^6 r_{14}^2 / [\varepsilon_{B,-1} L_{52}])^{1/4} \text{ GeV} \\ \epsilon_{p, \text{max}} &= \frac{q B' r}{2} \approx 5.5 \times 10^{11} \left(\frac{\varepsilon_{B,-1} L_{52}}{\varepsilon_{e,-1} \Gamma_{2.5}^2} \right)^{1/2} \text{ GeV}, \end{aligned} \quad (6)$$

respectively for $t'_{\text{acc}} = t'_{\text{syn}}$ and $t'_{\text{acc}} = t'_{\text{dyn}}$. For electrons, $t'_{\text{dyn}} \gg t'_{\text{syn}}$ typically and the maximum electron energy, using Eq. (6) for electrons, is $\epsilon_{e, \text{max}} \approx 10^6 \varepsilon_{e,-1.3}^{1/4} \varepsilon_{B,-1}^{-1/4} L_{52}^{-1/4} \Gamma_{2.5}^{3/2} r_{14}^{1/2} \text{ GeV}$.

At a given incident proton energy ϵ_p , the threshold photon energy leading to a Δ^+ resonance interaction is

$$\epsilon_{\gamma, \Delta^+} \simeq \frac{0.3 \Gamma^2}{(\epsilon_p / \text{GeV})} \text{ GeV}. \quad (7)$$

The optical depth for this interaction may be calculated using a delta-function approximation with a cross-section $\sigma_{p\gamma} \approx 10^{-28} \text{ cm}^2$ as

$$\tau'_{p\gamma}(\epsilon'_p) = \sigma_{p\gamma} \frac{r}{\Gamma} \left(\frac{dN'_{\gamma, \Delta^+}}{d\epsilon'_{\gamma, \Delta^+}} \right) d\epsilon'_{\gamma, \Delta^+} \quad (8)$$

using Eq. (5). Note that the target photon spectrum, within parenthesis, is now evaluated at the Δ^+ resonance energy [see Eq. (7)] for an incident proton energy ϵ'_p . In particular, Eq. (7) may be used to replace $\epsilon'_{\gamma, \Delta^+}$ by ϵ'_p in Eq. (5). As a result, the optical depth in Eq. (8) is expressed as a function of ϵ'_p . The spectral shape of the optical depth is then $\propto (\epsilon'_p)^{q-1}$, where q is the spectral index, $dN'_{\gamma}/d\epsilon'_{\gamma} \propto (\epsilon'_{\gamma})^{-q}$, in Eq. (5). Also the order is reversed, i.e. $q = 2, 1, -3/2$ in $\tau'_{p\gamma} \propto (\epsilon'_p)^{q-1}$ instead of $q = -3/2, 1, 2$ in $dN'_{\gamma}/d\epsilon'_{\gamma} \propto (\epsilon'_{\gamma})^{-q}$, according to the condition in Eq. (7).

Protons lose $\approx 20\%$ of their energy by $p\gamma$ interactions to π^0 and $\epsilon_{\gamma} \approx 0.1 \epsilon_p$ for each secondary photon. With an equal probability to produce π^0 and π^+ in each $p\gamma$ interaction, the resulting π^0 decay photon flux is

$$\frac{dN_{\gamma}}{d\epsilon_{\gamma}} = \min[1, \tau'_{p\gamma}] \frac{0.2 (\xi_p / \varepsilon_e) L_{\gamma}}{4 \pi d_L^2 \epsilon_{\gamma}^2}. \quad (9)$$

Here ξ_p is the proton fraction undergoing shock acceleration. For $\xi_p = 1$ and $\varepsilon_e = 0.05$ we have $\tau'_{p\gamma} \approx 1$ which leads to the observed flux level in Eq. (3). Secondary pions from Δ^+ decay, and subsequent decay photons and neutrinos follow the $dN_p/d\epsilon_p \propto \epsilon_p^{-p}$ spectral shape of the protons for a constant optical depth. For an optical depth of spectral shape $\propto \epsilon_p^{q-1}$, the resulting pion, photon and

neutrino spectra would be $dN/d\epsilon \propto \epsilon^{q-1-p}$. The π^0 decay photon spectrum in Eq. (9) is then $dN_\gamma/d\epsilon_\gamma \propto \epsilon_\gamma^{-2}$ between $\epsilon_\gamma = 0.03\Gamma^2/\epsilon_{\gamma,\text{pk}}$ GeV² and $0.03\Gamma^2/\epsilon_{\gamma,\text{sa}}$ GeV², $\propto \epsilon_\gamma^{-1}$ below $\epsilon_\gamma = 0.03\Gamma^2/\epsilon_{\gamma,\text{pk}}$ GeV² and $\propto \epsilon_\gamma^{-9/2}$ above $\epsilon_\gamma = 0.03\Gamma^2/\epsilon_{\gamma,\text{sa}}$ GeV² due to self-absorption following Eqs. (5) and (8).

Note that, the luminosity of shock-accelerated protons is $1/\epsilon_e = 20$ times the shock-accelerated electron luminosity. In the fast cooling scenario, valid in the GRB internal shocks, the electrons synchrotron radiate all their energy into observed γ -rays. Thus $L_p \approx L_\gamma/\epsilon_e$. In a single $p\gamma$ interaction the secondary pion (charged or neutral) luminosity is $L_\pi \approx 0.2L_p \approx 4L_\gamma/\epsilon_{e,-1.3}$. The neutrino luminosity of all flavors from charged pion decay, assuming equal energy for all 4 final leptons, is $L_\nu \approx (1/2)(3/4)L_\pi \approx 1.5L_\gamma/\epsilon_{e,-1.3}$. The 1/2 factor arises from the equal probability of π^0 and π^\pm production. The neutrinos carry away energy from the fireball, and the rest of the pion decay (e^+ from π^+ and $\gamma\gamma$ from π^0) energy is electromagnetic (e.m.), with a luminosity $L_{\text{e.m.}} \approx L_\pi - L_\nu \approx 2.5L_\gamma/\epsilon_{e,-1.3}$. A significant fraction of the π^0 -decay L_γ [Eq. (9)] would be converted to muon pairs and subsequently to neutrinos, as we discuss next. A substantial (small) fraction of the rest of $L_{\text{e.m.}}$ would be emitted at $r > r_{\text{ph}}$ ($r \approx r_{\text{ph}}$) as low energy photons with a luminosity not significantly above the observed γ -ray luminosity. These, however, do not affect substantially the neutrino flux calculated from very high energy γ -rays interacting with soft photons.

III. TWO PHOTON PAIR PRODUCTION

High energy γ -rays can produce lepton pairs, l^+l^- ($l = e, \mu$), with other photons which are above a threshold energy $\omega_{\text{th}} = m_l c^2$ in the center of mass (c.m.) frame of interaction. For an incident (target) photon of energy $\epsilon'_{\gamma,i}$ ($\epsilon'_{\gamma,t}$) in the comoving GRB fireball frame, $\omega = (2\epsilon'_{\gamma,i}\epsilon'_{\gamma,t})^{1/2}$, and the cross-section for l^+l^- pair production may be written, ignoring the logarithmic rise factor at high energy, as $\sigma_{\gamma\gamma \rightarrow l^+l^-} \approx \pi r_e^2 (m_l c^2/\omega)^2$, where r_e is the classical electron radius. The corresponding optical depth is

$$\tau_{\gamma\gamma}(\epsilon'_{\gamma,i}) = \frac{r}{\Gamma} \int \sigma_{\gamma\gamma}(\epsilon'_{\gamma,i}; \epsilon'_{\gamma,t}) \frac{dN'_{\gamma,t}}{d\epsilon'_{\gamma,t}} d\epsilon'_{\gamma,t}. \quad (10)$$

Given the power-law dependence of the photon distribution in Eq. (5), we may calculate the l^+l^- pair produc-

tion opacities by integrating Eq. (10) piecewise as

$$\tau_{\gamma\gamma \rightarrow l^+l^-}(\epsilon_\gamma) = r_e^2 m_e^2 c^3 L_\gamma / (8r \epsilon_{\gamma,\text{pk}}^2 \epsilon_\gamma) \times \begin{cases} \frac{1}{2} \left[\left(\frac{\epsilon_{\gamma,\text{pk}}}{\epsilon_{l,\text{th}}} \right)^2 - \left(\frac{\epsilon_{\gamma,\text{pk}}}{\epsilon_\gamma} \right)^2 \right]; \epsilon_\gamma < \frac{m_l^2 c^4 \Gamma^2}{2\epsilon_{\gamma,\text{pk}}} \\ \left(\frac{\epsilon_{\gamma,\text{pk}}}{\epsilon_{l,\text{th}}} - 1 \right) + \frac{1}{2} \left[1 - \left(\frac{\epsilon_{\gamma,\text{pk}}}{\epsilon_\gamma} \right)^2 \right]; \frac{m_l^2 c^4 \Gamma^2}{2\epsilon_{\gamma,\text{sa}}} > \epsilon_\gamma > \frac{m_l^2 c^4 \Gamma^2}{2\epsilon_{\gamma,\text{pk}}} \\ \frac{2}{3} \left(\frac{\epsilon_{\gamma,\text{pk}}}{\epsilon_{\gamma,\text{sa}}} \right) \left(1 - \frac{\epsilon_{l,\text{th}}}{\epsilon_{\gamma,\text{sa}}} \right)^{3/2} + \left(\frac{\epsilon_{\gamma,\text{pk}}}{\epsilon_{\gamma,\text{sa}}} - 1 \right) + \frac{1}{2} \left[1 - \left(\frac{\epsilon_{\gamma,\text{pk}}}{\epsilon_\gamma} \right)^2 \right]; \epsilon_\gamma > \frac{m_l^2 c^4 \Gamma^2}{2\epsilon_{\gamma,\text{sa}}} \end{cases} \quad (11)$$

Here we defined the threshold energy for lepton pair production as $\epsilon_{l,\text{th}} = m_l^2 c^4 \Gamma^2 / 2\epsilon_\gamma$. Note that the high energy photons produce e^+e^- pairs dominantly at lower energy. The ratio of the two opacities $\kappa = \tau_{\gamma\gamma \rightarrow \mu^+\mu^-} / \tau_{\gamma\gamma \rightarrow e^+e^-}$ becomes unity for higher energy photons, since the cross-section is the same for $\mu^+\mu^-$ and e^+e^- pair productions above the muon pair production threshold energy.

A. Muon decay neutrino flux

Muon pairs decay to neutrinos as $\mu^- \rightarrow e^- \bar{\nu}_e \nu_\mu$ and $\mu^+ \rightarrow e^+ \nu_e \bar{\nu}_\mu$ shortly after they are created in the c.m. frame of the $\gamma\gamma$ collision. In the observer's frame $\epsilon_\mu \approx \epsilon_\gamma/2$, and the particle pairs move radially along the incident photon's direction. For simplicity we assume that the ν_e and ν_μ created from μ -decay carry 1/3 of the muon energy each. The observed neutrino energies are then $\epsilon_\gamma/6$ for each flavor. The neutrino source flux, which is the same for ν_e , ν_μ , $\bar{\nu}_e$ and $\bar{\nu}_\mu$ previous to any flavor oscillation in vacuum, is

$$\epsilon_\nu \Phi_{\nu,\gamma\gamma}^s \equiv \epsilon_\nu \frac{dN_\nu}{d\epsilon_\nu} = \min[1, \tau_{\gamma\gamma \rightarrow \mu^+\mu^-}] \kappa \epsilon_\gamma \frac{dN_\gamma}{d\epsilon_\gamma}. \quad (12)$$

The high energy muons produced from $\gamma\gamma$ interactions may lose a significant fraction of their energy by synchrotron radiation before they decay into neutrinos (with a decay time t_{dec}), if their energy is above a break energy

$$\epsilon_{\mu,\text{sb}} = (6\pi m_\mu^5 c^5 \Gamma^2 / [t_{\text{dec}} \sigma_{\text{Th}} m_e^2 B'])^{1/2} \approx 5 \times 10^7 (\epsilon_{e,-1.3} \Gamma_{2.5}^4 r_{14}^2 / [\epsilon_{B,-1} L_{52}])^{1/2} \text{ GeV}. \quad (13)$$

The corresponding neutrino break energy from muon decay is $\epsilon_{\nu,\text{sb}} = \epsilon_{\mu,\text{sb}}/6$. For $\epsilon_\nu \gtrsim \epsilon_{\nu,\text{sb}}$, the neutrino flux index would steepen by a factor 2 [12].

We have plotted in Fig. 1 the ν_e flux at the source, $\epsilon_\nu^2 \Phi_\nu^s$ (same for ν_e , ν_μ , $\bar{\nu}_e$ and $\bar{\nu}_\mu$), previous to any vacuum oscillation, arising from $\gamma\gamma \rightarrow \mu^+\mu^-$ interactions and the associated muon decays, for a GRB of isotropic equivalent luminosity $L_\gamma = 10^{52}$ erg/s, which is average for a long GRB [5]. We assume a redshift of $z \sim 0.1$, which is near the low end of observed redshifts; there have been a few spectroscopic redshifts observed

in the 0.1 – 0.2 in the past 8 years, and indirect redshift measures, such as time lags, indicate many more bursts in this range among the BATSE sample (see, e.g., Ref. [5] and references therein). Also plotted are the ν_e source flux: $\epsilon_\nu^2 \Phi_\nu^s = \min[1, \tau'_{p\gamma}](0.2/8)L_\gamma/(4\pi d_L^2 \epsilon_e)$, from $p\gamma \rightarrow \Delta^+ \rightarrow n\pi^+$ interactions and subsequent π^+ and μ^+ decays. Different panels are for different bulk Lorentz factor Γ and dissipation radii r .

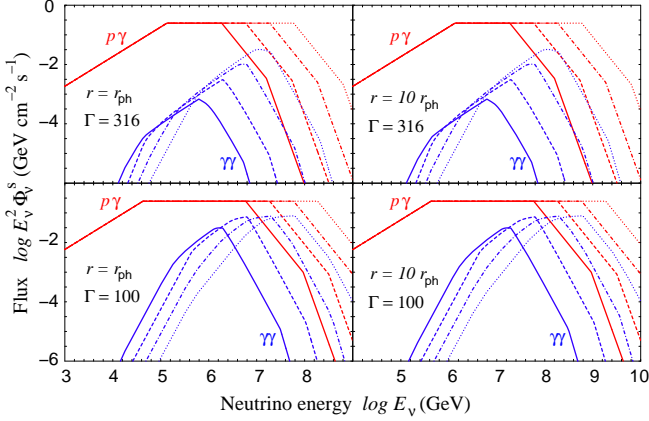


FIG. 1: Source flux of ν_e (same for ν_μ , $\bar{\nu}_e$ and $\bar{\nu}_\mu$) from $\gamma\gamma \rightarrow \mu^+\mu^-$ interaction and subsequent μ -decays, compared to the canonical ν_e flux (same for $\bar{\nu}_\mu$) from single $p\gamma \rightarrow n\pi^+$ interactions and subsequent π^+ , μ^+ decays. This is for a long duration GRB of $L_\gamma = 10^{52}$ erg/s at redshift $z \sim 0.1$. The solid, dashed, dot-dashed and dotted lines are for magnetic field parameters $\epsilon_B = 10^{-1}$, 10^{-2} , 10^{-3} and 10^{-4} respectively, for different Γ and r combinations.

B. Neutrino flavor oscillation and flux on Earth

While neutrinos are created via weak interactions as flavor eigenstates, their propagation is determined by the mass eigenstates. The flavor eigenstates ν_α and the mass eigenstates ν_j are mixed through a unitary matrix defined as $\nu_\alpha = \sum_j U_{\alpha j}^* \nu_j$, where $\alpha = e, \mu, \tau$ and $j = 1, 2, 3$ for three known flavors. The probability for flavor change by vacuum oscillation is given by $\mathcal{P}_{\nu_\alpha \rightarrow \nu_\beta} = \sum_j |U_{\beta j}|^2 |U_{\alpha j}|^2$, for the neutrino propagation from their sources to Earth over astrophysical distances.

We use the standard expression for $U_{\alpha,j}$ with solar mixing angle $\theta_\odot \equiv \theta_{12} = 32.5^\circ$ and atmospheric mixing angle $\theta_{\text{atm}} \equiv \theta_{23} = 45^\circ$ [13]. The unknown mixing angle θ_{13} and the CP violating phase may be assumed to be zero given the current upperbounds from reactor experiments. Using these values for $U_{\alpha,j}$ and $\mathcal{P}_{\nu_\alpha \rightarrow \nu_\beta}$ results in a relationship between the source neutrino fluxes Φ_ν^s and the expected neutrino fluxes on Earth Φ_ν , which is given by

$$\begin{bmatrix} \Phi_{\nu_e} \\ \Phi_{\nu_\mu} \\ \Phi_{\nu_\tau} \end{bmatrix} \approx \begin{bmatrix} 0.6 & 0.2 & 0.2 \\ 0.2 & 0.4 & 0.4 \\ 0.2 & 0.4 & 0.4 \end{bmatrix} \begin{bmatrix} \Phi_{\nu_e}^s \\ \Phi_{\nu_\mu}^s \\ \Phi_{\nu_\tau}^s \end{bmatrix}. \quad (14)$$

For antineutrinos $\mathcal{P}_{\bar{\nu}_\alpha \rightarrow \bar{\nu}_\beta}$ is the same as above.

Different production mechanisms produce ν and $\bar{\nu}$ fluxes at the source with different flavor proportions. Their production ratios may be expressed as normalized vectors, shown in the left hand side of Eqs. (15 & 16). The corresponding flux ratios at Earth, using Eq. (14), are shown in the right hand side of Eqs. (15 & 16) below

$$p\gamma \rightarrow n\pi^+ \quad \begin{bmatrix} \Phi_\nu^s \\ 1 \\ 1 \\ 0 \end{bmatrix} \quad \begin{bmatrix} \Phi_{\bar{\nu}}^s \\ 0 \\ 1 \\ 0 \end{bmatrix} \Rightarrow \begin{bmatrix} \Phi_\nu \\ 0.8 \\ 0.6 \\ 0.6 \end{bmatrix} \quad \begin{bmatrix} \Phi_{\bar{\nu}} \\ 0.2 \\ 0.4 \\ 0.4 \end{bmatrix}, \quad (15)$$

$$\gamma\gamma \rightarrow \mu^+\mu^- \quad \begin{bmatrix} \Phi_\nu^s \\ 1 \\ 1 \\ 0 \end{bmatrix} \quad \begin{bmatrix} \Phi_{\bar{\nu}}^s \\ 1 \\ 1 \\ 0 \end{bmatrix} \Rightarrow \begin{bmatrix} \Phi_\nu \\ 0.8 \\ 0.6 \\ 0.6 \end{bmatrix} \quad \begin{bmatrix} \Phi_{\bar{\nu}} \\ 0.8 \\ 0.6 \\ 0.6 \end{bmatrix}. \quad (16)$$

The source ν -fluxes plotted in Fig. 1 will be modified accordingly. Note that $\Phi_{\bar{\nu}_e}(\gamma\gamma)/\Phi_{\bar{\nu}_e}(p\gamma) \approx 4$ for the same initial $\gamma\gamma$ and $p\gamma$ flux levels. The $\bar{\nu}_e$ -flux component is 1/5 (1/15) of the total ν -flux from $\gamma\gamma$ ($p\gamma$). The observed ratio of $\bar{\nu}_e$ to total ν fluxes from both the single $p\gamma$ interactions and $\gamma\gamma$ interactions can be calculated using Eqs. (15 & 16) from the source fluxes as

$$\frac{\Phi_{\bar{\nu}_e}}{\Phi_\nu} = \frac{0.2\Phi_{\bar{\nu}_e,p\gamma}^s + 0.8\Phi_{\bar{\nu}_e,\gamma\gamma}^s}{3\Phi_{\bar{\nu}_e,p\gamma}^s + 4\Phi_{\bar{\nu}_e,\gamma\gamma}^s} \quad (17)$$

We have plotted this ratio in Fig. 2 for different GRB model parameters. The ratio is enhanced from the canonical ($p\gamma$) 1/15 value in the energy range where $\gamma\gamma$ interactions contribute significantly (see Fig. 1). Interestingly, the enhancement takes place over a small energy range which may be explored to learn about the GRB model parameters as we discuss next.

IV. NEUTRINO DETECTION

We consider here the anti-electron neutrino detection channel at the Glashow resonance energy $\epsilon_{\nu,\text{res}} = m_W^2 c^2 / 2m_e \approx 6.4$ PeV [8]. The number of electrons in the 2 km³ effective IceCube volume is $N_{e,\text{eff}} \approx 6 \times 10^{38}$ and the corresponding number of downgoing $\bar{\nu}_e$ events from a point source of flux $\Phi_{\bar{\nu}_e}$ is [4]

$$N_{\bar{\nu}_e} \approx \Delta t N_{e,\text{eff}} \frac{\pi g^2 (\hbar c)^2}{4m_e c^2} \Phi_{\bar{\nu}_e}(\epsilon_{\nu,\text{res}}). \quad (18)$$

Here $g^2 \simeq 0.43$ from the standard model of electro-weak theory, and Δt is the duration of the emission.

We have plotted in Fig. 3 the expected number of $\bar{\nu}_e$ events at $\epsilon_{\nu,\text{res}}$ from a GRB fireball for various value of r , ϵ_B and Γ . We have assumed here that shock accelerated protons interact once with synchrotron photons (two top panels), losing $\sim 20\%$ of their energy. For very high $p\gamma$ opacity the protons can lose most of their energy through

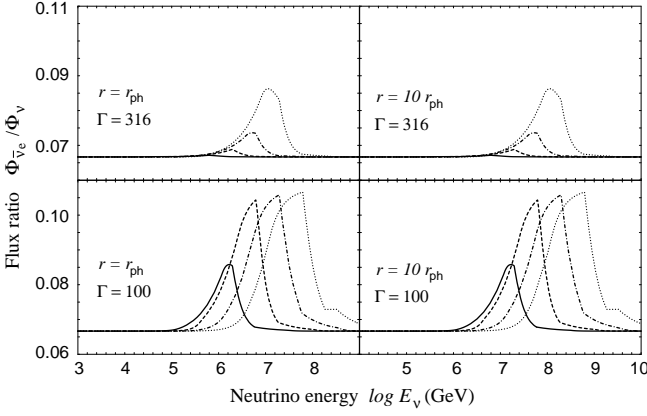


FIG. 2: Observed ratio of electron antineutrino flux to the total neutrino flux $\Phi_{\bar{\nu}_e}/\Phi_\nu$ for the $p\gamma$ and $\gamma\gamma$ source fluxes plotted in Fig. 1. This is for a long duration GRB of $L_\gamma = 10^{52}$ erg/s at redshift $z \sim 0.1$, the solid, dashed, dot-dashed and dotted lines indicate magnetic field parameters $\varepsilon_B = 10^{-1}, 10^{-2}, 10^{-3}$ and 10^{-4} respectively, for different Γ and r combinations. Note that the 1/15 ratio from single $p\gamma \rightarrow n\pi^+$ interactions is enhanced by $\gamma\gamma \rightarrow \mu^+\mu^-$ interactions in certain energy ranges which depend upon the GRB model parameters.

the $p\gamma$ and $n\gamma$ interaction chains. This could lead to the ν_e -fluxes from both $p\gamma$ and $\gamma\gamma$ plotted in Fig. 1 to roughly increase by a factor five. The $p\gamma$ source ν -fluxes may reach ratios $\Phi_\nu^s = \Phi_{\bar{\nu}}^s = [1, 2, 0]$, from π^+ and π^- decays, which at Earth would be $\Phi_\nu = \Phi_{\bar{\nu}} = [1, 1, 1]$ for $\varepsilon_\nu \lesssim \varepsilon_{\mu, \text{sb}}/2$. The resonant $\bar{\nu}_e$ -events in such case, from both $\gamma\gamma$ and $p\gamma$ fluxes, are plotted in Fig. 3 (two bottom panels). For simplicity, we assumed $\Phi_\nu \propto \Phi_\gamma \propto \min[1, 0.2\tau'_{p\gamma}]$ for the $p\gamma$ ν -flux and γ -flux in Eq. (12). Also $\Phi_{\bar{\nu}} = [1, 1, 1]$ from $p/n\gamma$ interactions for $\tau'_{p\gamma} \geq 2$.

The background for astrophysical $\bar{\nu}_e$ detection is mostly due to atmospheric prompt neutrinos from cosmic-ray generated charm meson decays. A parametrization for the ν_e and $\bar{\nu}_e$ atmospheric flux is given by [15]

$$\Phi_{\nu_e + \bar{\nu}_e}^{\text{atm}} = \begin{cases} \frac{1.5 \times 10^{-5} \varepsilon_\nu^{-2.77}}{1 + 3 \times 10^{-8} \varepsilon_\nu^{-8}}; & \varepsilon_\nu < 1.2 \times 10^6 \text{ GeV} \\ \frac{4.9 \times 10^{-4} \varepsilon_{\nu, \text{ob}}^{-3.02}}{1 + 3 \times 10^{-8} \varepsilon_\nu^{-8}}; & \varepsilon_\nu > 1.2 \times 10^6 \text{ GeV} \end{cases} \times \text{GeV}^{-1} \text{ cm}^{-2} \text{ s}^{-1} \text{ sr}^{-1}. \quad (19)$$

The corresponding background $\bar{\nu}_e$ -events at the Glashow resonance energy is $\lesssim 10^{-7}$ for a GRB within a ~ 100 s time window, allowing the full directional uncertainty (2π sr), given the poor current knowledge of the ν_e or $\bar{\nu}_e$ signal reconstruction in neutrino Cherenkov detectors, from Eq. (18).

V. DISCUSSION

The results of Fig. 3 and Eqs. (15 & 16) show that $\gamma\gamma$ interactions in astrophysical sources can enhance the

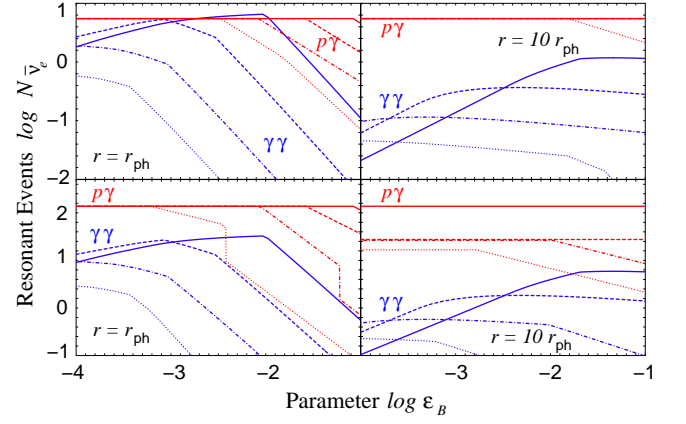


FIG. 3: Resonant $\bar{\nu}_e$ events in IceCube from $\gamma\gamma$ and $p\gamma$ interactions in a GRB, as a function of the magnetization ε_B for Lorentz factor Γ of 100 (solid lines), 178 (dashed lines), 316 (dot-dashed lines), 500 (dotted lines) and fireball radii equal to the photospheric radius (*two left panels*) and ten times the photospheric radii (*two right panels*). We used single $p\gamma$ interactions (*two top panels*) and multiple $p\gamma$ and subsequent $n\gamma$ interactions proportional to $\tau_{p\gamma}$ (*two bottom panels*) for comparison. Other GRB parameters are $z = 0.1$, $\Delta t = 30$ s, $L_\gamma = 10^{52}$ erg/s and $\varepsilon_e = 0.05$.

observed $\Phi_{\bar{\nu}_e} : \Phi_\nu$ flux ratio. A different source of enhancement of the $\bar{\nu}_e$ flux may be pp interactions [3, 4]. In GRBs, however, the optical depth to pp is low [7], except in buried jets leading to ν precursors [14], where pp interactions are expected to lead to ν 's at energies \sim TeV. The number of resonant $\bar{\nu}_e$ events arising from $p\gamma$ interactions is essentially independent of ε_B (for $\varepsilon_B \lesssim 10^{-2}$) for any Γ . On the other hand, the number of resonant $\bar{\nu}_e$ events arising from $\gamma\gamma$ interactions varies significantly with Γ and r . It may become as large as the $p\gamma$ contribution for $10^{-2} \lesssim \varepsilon_B \lesssim 10^{-3}$, $100 \lesssim \Gamma \lesssim 300$ and $r_{\text{ph}} \lesssim r \lesssim 3r_{\text{ph}}$. For long bursts of average isotropic-equivalent luminosity at a redshift ~ 0.1 , which from past experience are electromagnetically detected every few years, IceCube could probe the $\bar{\nu}_e$ enhancement, and thus the value of the magnetization parameter and dissipation radius, by measuring the $\Phi_{\bar{\nu}_e} : \Phi_\nu$ flux ratio. Finally, we note that a moderate excess of ν_e events compared to ν_μ and ν_τ events may also be an indication for the presence of a $\gamma\gamma$ component.

Acknowledgements

Work supported by NSF grant AST0307376. EW is partly supported by Minerva and ISF grants.

-
- [1] T. K. Gaisser, Nucl. Phys. Proc. Suppl. **117**, 318 (2003);
E. Waxman, Proc. Nobel Symp. 129: Neutrino Physics
(Sweden 2004), [arXiv:astro-ph/0502159].
 - [2] J. G. Learned and S. Pakvasa, Astropart. Phys. **3**, 267
(1995).
 - [3] T. Kashti and E. Waxman, Phys. Rev. Lett. **95**, 181101
(2005) [arXiv:astro-ph/0507599].
 - [4] L. A. Anchordoqui, H. Goldberg, F. Halzen and
T. J. Weiler, Phys. Lett. B **621**, 18 (2005)
[arXiv:hep-ph/0410003].
 - [5] B. Zhang and P. Mészáros, Int. J. Mod. Phys. A **19**,
2385 (2004).
 - [6] E. Waxman, Phys. Rev. Lett. **75**, 386 (1995)
 - [7] E. Waxman and J. N. Bahcall, Phys. Rev. Lett. **78**, 2292
(1997).
 - [8] S. L. Glashow, Phys. Rev. **118**, 316 (1960).
 - [9] J. Ahrens *et al.*, Astropart. Phys. **20**, 507 (2004).
 - [10] D. Band, *et al.*, 1993, Astrophys. J. **413**, 281 (1993).
 - [11] S. Razzaque, P. Mészáros and B. Zhang, Astrophys. J.
613, 1072 (2004). Note a (typo) missing power index
 $p + 2$ on $(B' \sin \theta)$ in the expression of Eq. (8) in this
paper.
 - [12] J. P. Rachen and P. Mészáros, Phys. Rev. D **58**, 123005
(1998).
 - [13] S. Eidelman *et al.*, Phys. Lett. B **592**, 1 (2004).
 - [14] S. Razzaque, P. Mészáros and E. Waxman, Phys. Rev. D
68, 3001 (2003)
 - [15] M. Thunman *et al.*, Astropart. Phys. **5**, 309 (1996).